Micromagnetic simulation of domain structures in patterned magnetic tunnel junctions

T. Schrefl[a] and J. Fidler
Institute für Angewandte und Technische Physik, Vienna University of Technology, Wiedner Hauptstrasse 8-10, A-1040 Vienna, Austria

J. N. Chapman and K. J. Kirk
University of Glasgow, Department of Physics and Astronomy, Glasgow, Scotland, G128QQ, United Kingdom

The magnetization reversal process of patterned magnetic tunnel junctions was investigated using finite element micromagnetics, taking into account the magnetostatic interactions between the pinned and the free layer. Two different reversal modes were observed in the simulations depending on the domain structure for zero applied field. In order to reduce the magnetostatic energy, end domains form in the free layer either in the *S* state or the *C* state. If the system is in the *S* state, the end domains grow under the influence of a reversed field. The end domains touch each other, leading to the reversal of the center. Finally, the residual domains along the edges parallel to the field direction reverse. If the system is in the *C* state, the growth of the end domains leads to a four domain flux closure structure. The domain with the magnetization in favor of the field direction expands until the free layer becomes reversed at a field. The *S* state and the *C* state were found to differ in energy by less than 0.2%. © *2001 American Institute of Physics.*
[DOI: 10.1063/1.1360329]

I. INTRODUCTION

Magnetic multilayer films which show electron-spin dependent transport are used in sensing and storage devices. A promising system for application in magnetic random access memory is spin-tunnel junctions.[1] With decreasing lateral size of the elements the uniformity of the magnetization and its influence on the tunneling behavior becomes important. Recently, Ardhuin[2] and coworkers investigated the magnetization reversal of the free layer using Lorentz microscopy in the transmission electron microscope. Under the influence of a field parallel to the bias direction, elongated elements are found to reverse by the growth and subsequent annihilation of a quasiperiodic domain structure which evolves from the ends of the element. This process is the same in both halves of the magnetization cycle. The reversal of square elements involves the formation of more complex domain structures which differ significantly according to the direction in which the field is applied. Zhu and coworkers[3] numerically investigated the influence of the shape on the magnetization reversal of pseudo-spin valve structures. In elongated elements with flat ends the switching process starts from the end, leading to nonreproducable domain patterns and switching fields. In elements with tapered ends, magnetization starts to rotate in the center of the element, causing a well-defined switching process. Koch and coworkers[4] investigated the switching dynamics of micron-sized magnetic thin films experimentally and numerically. They observed switching times well below 500 ps.

This work uses a finite element technique to calculate the domain structures during the magnetization reversal of the free layer of a patterned spin-tunnel junction. The magnetostatic interactions between the free and the pinned layer are an inherent part of the simulation model.

II. MICROMAGNETICS AND THE MODEL SYSTEM

Figure 1 shows the finite element model used for the simulations. The model consists of a free NiFe layer with a thickness of 10 nm and an extension of 500×500 nm. The free layer is placed above the center of a 1000×1000 nm wide pinned layer. The distance between the layers is 1.5 nm. Both layers are subdivided into tetrahedral finite elements. The element size within the free layer and the pinned layer is 5 and 20 nm, respectively. The magnetostatic interactions between the layers are simulated using a hybrid finite element/boundary element method.[5] Thus no mesh is required outside the ferromagnetic layers. Table I gives the intrinsic magnetic properties of the free and the pinned layer. We assume zero magnetocrystalline anisotropy.

The equilibrium distribution of the magnetization for different applied fields is obtained from the solution of the Gilbert equation of motion. The Gilbert damping constant was varied between $\alpha=0.1$ and $\alpha=1$. Whereas the switching fields where found to decrease with decreasing damping

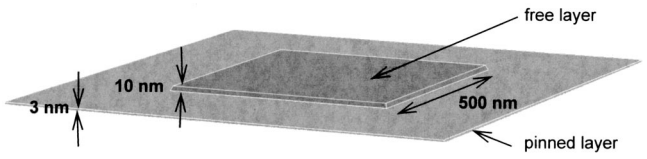

FIG. 1. Finite element model of a patterned magnetic tunnel junction. The free layer is placed above the center of the pinned layer.

[a]Electronic mail: thomas.schrefl@tuwien.ac.at

TABLE I. Intrinsic magnetic properties used for the calculations. The saturation polarization J_S, the exchange constant A, the pinning field H_p, and the film thickness t.

	J_S (T)	A (pJ/m)	H_p (kA/m)	t (nm)
free layer	1.0	10	0	10, 15, 20
pinned layer	1.4	13	25–42	3

constant, no significant change was observed in the magnetization reversal process for small and large damping.

III. REMANENT STATES

Small ferromagnetic thin film elements show different equilibrium states depending on the magnetic history of the sample. Once a thin film element has been saturated the magnetization near the edges rotates parallel to the surface in order to reduce the magnetostatic energy. If the magnetization in both end domains is parallel to each other the magnetization forms an ''S-shape'' configuration. If the magnetization along the edges is oppositely directed, the magnetization forms a ''C-shape'' configuration. Figure 2 gives the domain structure in the *S* state and the *C* state. In addition, the magnetization distribution within the pinned layer is plotted for a pining field of $H_p = 36$ kA/m. The results clearly show that the magnetic surface charges at the edges of the free layer cause magnetic volume charges within the pinned layer which again may influence the magnetization distribution of the free layer.

Figure 3 compares the total energy of the different remanent states for different values of the pinning field. If the magnetization of the free and the pinned layer are oppositely directed, the energy of the *C* state is lower than the energy of the *S* state. If the magnetization of both layers was originally parallel, the *C* state shows a lower energy for a wide range of

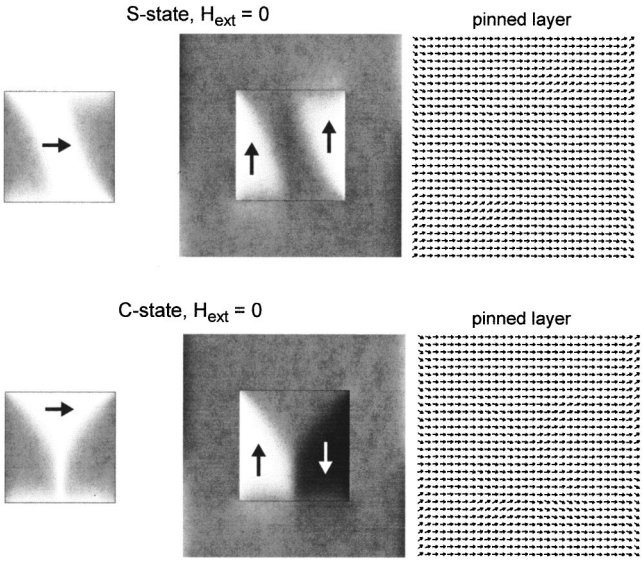

FIG. 2. Magnetization configuration in the *S* state and in the *C* state. The grayscale maps the magnetization component parallel (left-hand side) and normal (right-hand side) to the bias direction. The arrows indicate the magnetization distribution in the pinned layer. For the calculation a pinning field $H_p = 36$ kA/m was used.

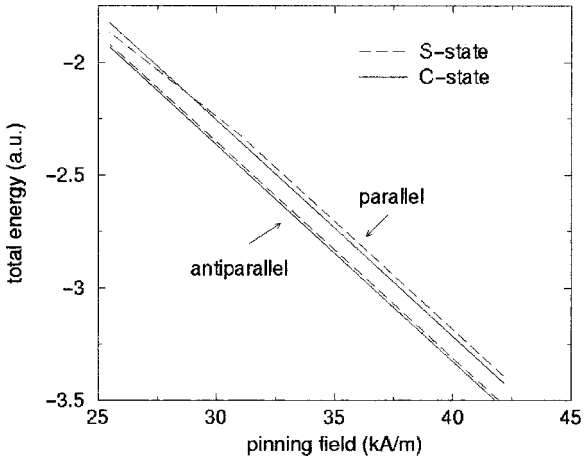

FIG. 3. Total energy of the remanent states as a function of the pinning field H_p. The dashed and the solid lines refer to the *S* state and the *C* state, respectively. The upper two lines correspond to configurations where the magnetization of the free and pinned layer are parallel, the lower two lines give the result for antiparallel magnetization.

the pinning field. The energy of the *S* state becomes smaller than that of the *C* state for a pinning field of $H_p = 25$ kA/m. This result clearly shows that magnetostatic interactions mutually influence the magnetization distribution of the different layers. For all investigated configurations, the energy of both states differ by less than 0.2%.

IV. FREE LAYER REVERSAL

The micromagnetic simulations show that two distinct reversal mechanisms are possible depending on the magnetization configuration for zero applied field. The saturated state with the magnetization of the pinned and the free layer parallel to the bias direction was the initial state for the computer experiments. If the saturation field is applied under an angle of 10° with respect to the bias direction and continuously decreased, the system will form an *S* state for zero applied field. A saturation field strictly parallel to the bias direction will lead to the *C* state. Once the system is in the *S* state, the system will end up in an *S* state after a complete magnetization cycle, although complex domain structures are formed during reversal. Similarly a system being originally in the *C* state will arrive in a *C* state after magnetization reversal. However, magnetostatic interactions between the pinned and the free layer may eventually cause a transition from the *C* state to the *S* state if the pinning field is low.

Figure 4 shows the domain patterns during magnetization reversal starting from the *S* state with the magnetization of both layers directed originally parallel and a free layer thickness of 10 nm. The end domains grow under the influence of a reversed field. At a field of 1.6 kA/m the end domains touch each other, leading to the reversal of the center. Finally, the residual domains along the edges parallel to the field direction reverse at a field of 5.5 kA/m. Figure 5 gives the domain structure which is involved during the reversal starting from the *C* state, where the magnetization of both layers was originally parallel to the bias direction and a free layer thickness of 10 nm. Again the end domains grow under the influence of the reversed field. After formation of a

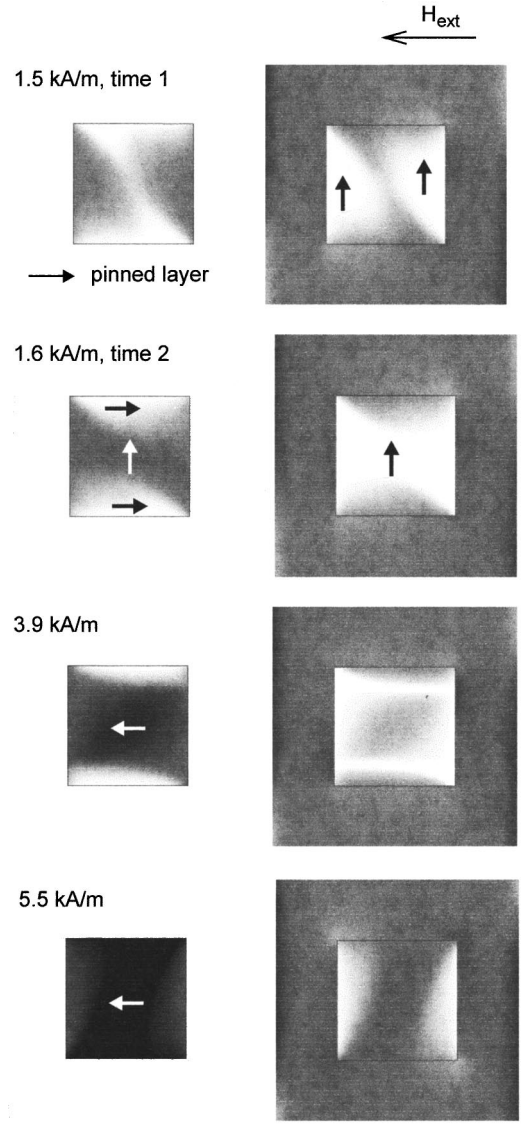

FIG. 4. The domain patterns for different fields and different times during magnetization reversal starting from the *S* state. The grayscale maps the magnetization component parallel (left-hand side) and normal (right-hand side) to the bias direction.

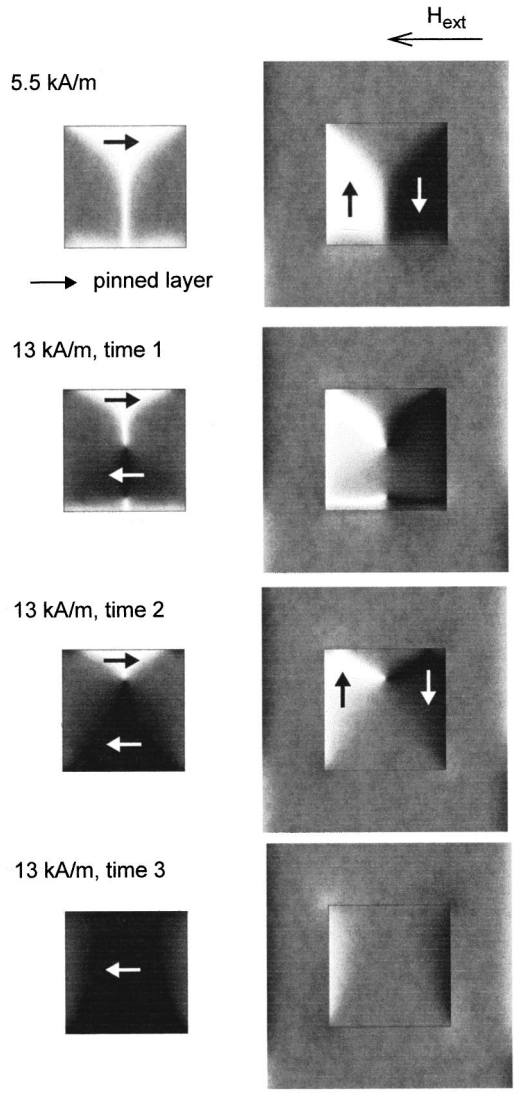

FIG. 5. The domain patterns for different fields and different times during magnetization reversal starting from the *C* state. The grayscale maps the magnetization component parallel (left-hand side) and normal (right-hand side) to the bias direction.

complex domain structure, a four domain flux closure pattern is formed. The domain with the magnetization in favor of the field direction expands until the free layer becomes reversed at a field of 13 kA/m. Similar reversal processes are observed for the second half of the magnetization cycle. The field required to switch the magnetization of the *C* state is about twice as large as the switching field of the *S* state. The switching field depends considerably on the thickness of the free layer *t*. If *t* is increased from 10 to 20 nm, the switching field of the *S* state increases from 5.5 to 8 kA/m whereas the switching field of the *C* state decreases from 13 to 5.2 kA/m.

V. CONCLUSIONS

Numerical micromagnetic calculations show that the energy of different remanent states is rather similar. The difference between the energy of the *S* state and the energy of the *C* state is less than 0.2%. Depending on the magnetization configuration within the pinned layer, either of the two states could have the lower energy. In real devices structural inhomogeneities and thermal fluctuations may determine the magnetic state and the reversal mechanism.

ACKNOWLEDGMENT

This work was supported by the Austrian Science Fund (Project No. Y132-PHY).

[1] S. S. Parkin *et al.*, J. Appl. Phys. **85**, 5828 (1999).
[2] H. Ardhuin *et al.*, J. Appl. Phys. **88**, 2760 (2000).
[3] T. N. Fang and J. G. Zhu, J. Appl. Phys. **87**, 7061 (2000).
[4] R. H. Koch *et al.*, Phys. Rev. Lett. **81**, 4512 (1998).
[5] D. R. Fredkin and T. R. Koehler, IEEE Trans. Magn. **26**, 415 (1990).